TN-20
197735
27p.

NASA TN D-203

TECHNICAL NOTE

D-203

EXPERIMENTAL STUDY OF ZERO-FLOW EJECTORS USING GASEOUS NITROGEN

By William L. Jones, Harold G. Price, Jr.
and Carl F. Lorenzo

Lewis Research Center
Cleveland, Ohio

NATIONAL AERONAUTICS AND SPACE ADMINISTRATION

WASHINGTON

March 1960

(NASA-TN-D-203) EXPERIMENTAL STUDY OF ZERO-FLOW EJECTORS USING GASEOUS NITROGEN (NASA) 27 p

N89-70603

Unclas
00/20 0197735

NATIONAL AERONAUTICS AND SPACE ADMINISTRATION

TECHNICAL NOTE D-203

EXPERIMENTAL STUDY OF ZERO-FLOW EJECTORS USING GASEOUS NITROGEN

By William L. Jones, Harold G. Price, Jr.
and Carl F. Lorenzo

E-485

CQ-1

SUMMARY

Experimental models of two zero-flow ejector types were studied to determine the factors important in the design of such ejectors for altitude testing of rocket engines. The investigation covered both straight-tube and second-throat ejector types, and used both bell-shaped and 15°-conical primary nozzles having area ratios of 25:1. A second 15°-conical primary nozzle having an area ratio of 50:1 was also used. Both ejector types were investigated over a range of area ratios and length-to-diameter ratios. Second-throat ejectors were investigated at several contraction angles.

A chamber-to-ambient starting-pressure ratio of about 23 was required to provide full nozzle flow for both bell and conical 25:1-area-ratio nozzles operating with a straight-tube ejector having a length-to-diameter ratio of 8 and an ejector-to-nozzle-throat area ratio of 28. A reduction from 23 to 13.5 in chamber-to-ambient starting-pressure ratio for full nozzle flow was obtained by use of a second-throat ejector having a 6° contraction angle, a contraction area ratio of 2.14, and a second-throat length-to-diameter ratio of 6.0.

Experimental maximum ejector contraction area ratios and starting performance are given for a range of ejector inlet Mach numbers from 1 to 10.

INTRODUCTION

Rocket engines having large-area-ratio exhaust nozzles are of prime interest for outer atmosphere and space vehicles. Performance evaluation of these engines at sea-level exhaust pressure provides only off-design data. Evaluation of performance at the design altitude may be accomplished in an altitude facility, but the exhaust flow and cooling limitation of currently available facilities impose serious limitations on the size or thrust level of the rocket engine that may be tested. Another method of providing low exit engine pressure is by utilizing the high

kinetic energy of the rocket exhaust to drive a zero-flow ejector device. Ejector devices do not restrict the size of the engine; the only restriction imposed is that of a sufficient primary-stream pressure ratio.

The term "zero-flow ejector" is used to denote a shroudlike device that attaches to the exit of a primary convergent-divergent nozzle. The device utilizes the high kinetic energy of the primary stream, by supersonic diffusion, to provide a reduction in the primary-nozzle back pressure. A description of the ejector-flow process is given in RESULTS AND DISCUSSION. A theory for predicting the performance of cylindrical ejectors is given in reference 1.

E-485

Inasmuch as the flow process of the zero-flow ejector is similar to supersonic-diffuser devices, the results of several diffuser experiments are included for comparison. These results (refs. 2 to 5) were obtained with two-dimensional supersonic diffusers in the Mach number range 1.9 to 9.6. The present investigation, in the Mach number range from about 5 to 6, was conducted with small-scale, fixed-geometry cylindrical and conical zero-flow ejectors to determine their performance and optimum design for use with rocket engines. This Mach number range corresponds to an area-ratio range of approximately 25 to 55 for nitrogen gas (used for this investigation), or about 25 to 150 for rocket engines using a wide variety of propellants.

Two general types of ejectors were studied: the straight-tube ejector and the second-throat ejector. Two 25:1-area-ratio primary nozzles were used with each ejector type: a bell shape, and a 15° conical. A 50:1-area-ratio 15°-conical nozzle was also used with several ejector configurations. The straight-tube ejectors were studied over a range of ejector-to-nozzle-throat area ratios from 28 to 51 and a range of ejector length-to-diameter ratios from 2 to 16. Second-throat ejectors were studied over a range of contraction area ratios from 1.66 to 2.49, contraction angles from 3° to 15°, and overall-length-to-diameter ratios from about 2 to 11. The investigation covered a range of chamber-to-ambient pressure ratios from about 10 to 48.

SYMBOLS

The following symbols are used in this report:

A	cross-sectional area
D	maximum diameter
d	minimum diameter
L	overall length

E-485

CQ-1 back

l	second-throat length
M	Mach number
P	total pressure
$(P_c/P_0)_{min}$	minimum starting and operating ejector pressure ratio
p	static pressure
s	spacing
γ	specific heat ratio
δ	contraction angle
ϵ	nozzle area ratio, $A_e/A_{t,1}$
θ	subsonic-diffuser angle
ψ	contraction area ratio, $A_{ej}/A_{t,2}$

Subscripts:

c	chamber
e	exit
ej	ejector
n	nozzle
t	throat
0	ambient
1	nozzle throat
2	second throat
3	subsonic-diffuser exit

APPARATUS AND PROCEDURE

Test Equipment

The test equipment included a chamber and a primary nozzle to which a series of ejector configurations could be attached (fig. 1). Provisions were made for changing primary nozzles as well as ejector configurations.

Two 15°-conical nozzles having area ratios of 25:1 and 50:1 and a bell-shaped 25:1-area-ratio nozzle were used. The bell-shaped nozzle had a length equal to 80 percent of the 15°-conical nozzle, with a 4° divergent angle at the exit. All nozzles had throat diameters of 0.26 inch. Nitrogen gas supplied by a high-pressure bottle system was used as the working fluid. Nozzle and ejector pressures were measured by using a mercury manometer system.

Ejector Configurations

Straight-tube ejectors. - Three tubes of different diameters having sufficient length to permit investigation of length-to-diameter ratios up to 16 were used. A 2:1-area-ratio subsonic diffuser was provided for attachment to the end of each straight tube.

Second-throat ejectors. - Second-throat ejectors incorporated segmented construction that permitted interchanging of the various nozzle and ejector configurations. The ejector configurations permitted variation of ejector spacing, contraction angle, contraction area ratio, and second-throat length-to-diameter ratio (see fig. 2).

A list of all the configurations for both straight-tube and second-throat ejectors investigated is given in table I.

Procedure

Ejector data were obtained by increasing chamber pressure (thereby increasing chamber-to-ambient pressure ratio) in steps from a low value up to about 48 atmospheres. Hysteresis effects were determined by decreasing chamber pressure in steps from about 48 atmospheres down to low values. At each value of chamber pressure, the chamber, nozzle exit, and ejector pressures were recorded by photographing a gage and manometer system. A mercury barometer was used to determine the atmospheric or ambient pressure.

Straight-tube ejectors were studied over a range of ejector-to-nozzle-throat area ratios from 28 to 51 and over a range of ejector length-to-diameter ratios from 2 to 16. Ejector performance was also evaluated both with and without a 2:1-area-ratio subsonic diffuser.

Second-throat ejectors were investigated over a range of contraction area ratios from 1.66 to 2.48 for contraction angles of 3°, 6°, and 15°. Ejector spacing-to-diameter ratio was varied from 0 to 3.2, and second-throat length-to-diameter ratio was varied from 0 to 10. A 2:1-area-ratio subsonic diffuser was used with all second-throat configurations.

RESULTS AND DISCUSSION

Ejector and nozzle starting and hysteresis effects are illustrated by typical ejector performance curves in figures 3 and 4. As the overall pressure ratio P_c/P_0 of the nozzle-ejector combination is increased from a low value, first the nozzle and then the ejector start. The term "start" is used to define the region where a constant nozzle or ejector pressure ratio (p_n/P_c or p_{ej}/P_c) exists. This region corresponds to full or attached supersonic flow in the nozzle and in the ejector. Experimental evidence (nozzle exit and ejector pressures) indicates that the free-stream expansion occurring after the full-flowing supersonic nozzle in a full-flowing ejector occurs at nearly the isentropic value corresponding to the expansion ratio. This occurrence can be explained theoretically (ref. 1) by a Prandtl-Meyer expansion at the nozzle exit. As the expanded flow then comes into contact with the ejector tube wall, an attached shock system is produced. This shock system extends several tube diameters downstream before completion (ref. 6).

The minimum starting-pressure ratio P_c/P_0 obtained by increasing P_c/P_0 is defined as the lowest value that results in constant p_n/P_c or p_{ej}/P_c (figs. 3 or 4). After ejector starting has occurred, a region extending to a somewhat lower value of P_c/P_0 may exist for certain ejector types (see fig. 4). This region, which includes the start region, is called "operate" and is obtained by decreasing P_c/P_0. The difference between the minimum start and minimum operate points is a result of hysteresis effects that are present, depending upon nozzle and ejector design.

A region of instability exists between points of minimum start for the nozzle and for the ejector (fig. 3). Operation in this region results in pressure fluctuations and loud buzzing noise. Stable operation of the ejector-nozzle combination then was restricted to the start and operate regimes associated with the ejector.

Straight-Tube Ejectors

The effect of ejector-to-nozzle-throat area ratio $A_{ej}/A_{t,1}$ on the minimum ejector starting-pressure ratio P_c/P_0 for all straight-tube ejectors investigated is shown in figure 5. Data are shown for ejector area ratios from 28:1 to 51:1 for the bell and conical 25:1-area-ratio nozzles, and a single point is included for the 51:1-area-ratio ejector with a 50:1-area-ratio conical nozzle. Two theoretical curves are also presented, one with subsonic diffusion and the other without. These

curves were calculated from one-dimensional theory (ref. 7), assuming normal shock recovery with and without 2:1-area-ratio subsonic diffusion. The effect of nozzle contour and of nozzle area ratio on ejector starting performance is illustrated by the data for the 51:1-area-ratio ejector. The 25:1- and 50:1-area-ratio conical nozzles operating with the 51:1-area-ratio ejector gave nearly the same ejector starting-pressure ratio. The bell nozzle operating with the 51:1-area-ratio ejector required a somewhat higher pressure ratio than the conical nozzles.

Because of the relatively small effects of nozzle contour and nozzle area ratio on the straight-tube ejector starting performance, the experimental curves presented in figure 5 can be used with reasonable accuracy for gases with a specific heat ratio of 1.4 to predict the starting performance of any ejector-nozzle combination from low values of ejector area ratio to values of 50:1 or higher. In designing an ejector to operate with any rocket exhaust nozzle, the best starting or operating pressure ratio is always obtained with an ejector of approximately the same area ratio as the nozzle itself. In the present investigation, it was deemed desirable that the minimum ejector size be slightly larger than the nozzle itself in order to minimize the possibility of nozzle-ejector interactions. The data of figure 5 are, however, useful to predict performance of nozzle-ejector combinations not only for the case where the ejector and nozzle are of similar size but for ejector-nozzle combinations where the ejector tube is much larger than the nozzle.

The effect of ejector overall-length-to-diameter ratio L/D_{ej} on P_c/P_0 for the three ejectors investigated is shown in figure 6. Data are shown for a range of length-to-diameter ratios from 2 to 16 for both bell and conical nozzle and with and without a 2:1-area-ratio subsonic diffuser.

The minimum chamber-to-ambient starting-pressure ratio occurred at overall-length-to-diameter ratios between 8 and 10 for all configurations investigated. Higher starting-pressure ratios were required for the bell nozzle with the 51:1-area-ratio ejector at all length-to-diameter ratios than were required for the conical nozzle and the 51:1-area-ratio ejector. By use of a 2:1-area-ratio subsonic diffuser with the 28:1-area-ratio ejector, the same starting performance could be obtained at an overall length-to-diameter ratio of about 5.5 as was obtained without the diffuser at an overall length-to-diameter ratio of 10. Similar effects with the subsonic diffuser are shown for the 33:1- and 51:1-area-ratio ejectors.

Second-Throat Ejectors

The spacing between the second-throat contraction and the nozzle for each configuration is a factor that determines whether the ejector-nozzle

combination can be started. To avoid possible interaction between the ejector and nozzle, it was deemed desirable to provide some distance between the plane of the nozzle exit and the beginning of the second-throat contraction. The effect of this distance, or ejector spacing ratio s/D_{ej}, on p_n/P_c for three typical second-throat ejectors with both bell and conical nozzles is presented in figure 7 (p_n/P_c is used to indicate whether the nozzle is flowing full).

At a maximum spacing ratio of about 0.2, all ejector configurations could be started. This maximum value of spacing ratio was then used for all subsequent ejector configurations reported herein.

Typical ejector performance curves to show the effect of variation of second-throat length-to-diameter ratio on ejector starting- and operating-pressure ratio are presented in figure 8. Minimum ejector starting-pressure ratios with the conical nozzle occurred at length-to-diameter ratios between 5 and 7 for all ejector configurations investigated. Minimum ejector operating pressures, however, occurred at length-to-diameter ratios 9 to 10. In general, starting- and operating-pressure ratios for the conical nozzle were about doubled when the second-throat length-to-diameter ratio was reduced from about 6 to zero. Starting-pressure ratios with the bell nozzle (fig. 8(b)) were not improved as much with the addition of ejector throat length as were the starting-pressure ratios with the conical nozzle. Considerable improvement in the minimum operating-pressure ratio, however, was obtained by the addition of second-throat length. The lowest operating-pressure ratio, about 14.0, occurred at the maximum length-to-diameter ratio investigated. This maximum value of $l/d_{t,2}$ also corresponds to the highest starting-pressure ratio, about 24.0, and is about equal to the starting-pressure ratio for an $l/d_{t,2}$ of zero.

The effect of variation of ejector overall-length-to-maximum-diameter ratio on the minimum starting and operating pressure ratios for the conical nozzle is shown in figure 9. The configuration with contraction angles δ of 6° exhibited the most desirable characteristics on the basis of length and starting and operating pressure ratios. The optimum contraction area ratio resulted in the maximum value of 2.14 that could be started; however, within the range investigated (ψ = 1.66 to 2.14), the effect of variation of ψ was small. The minimum starting-pressure ratio corresponding to the optimum configuration was 13.5.

Similar effects on ejector performance (although occurring at higher pressure ratios) of variation of L/D_{ej} for the bell nozzle are illustrated in figure 10. The minimum starting-pressure ratio for δ of 3° (fig. 10(a)) occurred at L/D_{ej} of about 5. The minimum operating-pressure ratio, however, would require L/D_{ej} of 10 or greater. For δ

of 15° (fig. 10(b)), the minimum starting- and operating-pressure ratios were nearly the same and occurred at an L/D_{ej} of about 6.

Maximum ejector contraction ratio for starting as a function of ejector inlet Mach number is shown in figure 11. Experimental data are presented both from the present investigation and from diffuser investigations with two-dimensional tunnels (refs. 3 to 5). Experimental data obtained in the present investigation are shown for second-throat ejectors with 25:1- and 50:1-area-ratio conical nozzles. A theoretical curve is included for the maximum theoretical contraction ratio for starting based on a normal shock at the ejector inlet for a specific heat ratio γ of 1.4. The γ of the expanded exhaust gases of most rocket engines is less than 1.4. At these lower γ values, the theoretical ψ_{max} is increased. Although no data were obtained experimentally for the maximum value of ψ at high temperatures or with gases having other than γ of 1.4, an ejector with a ψ value of 2.14 was successfully started using a hot firing rocket (fig. 11). The γ value for the expanded exhaust gas of this rocket was between 1.3 and 1.4 ($A_{ej}/A_{t,1} = 28.2$). The maximum value of ψ for rocket engines with conical nozzles may be somewhat greater than the experimental curve shown in figure 11. Therefore, this curve should give conservative values for use in the design of ejectors for rocket engines with conical nozzles.

A single point is shown in figure 11 for the maximum value of ψ for an ejector with the bell nozzle. It is believed that the lower value of ψ_{max} obtained for the bell nozzle was due to possible higher total-pressure starting losses associated with this short nozzle design.

Ejector minimum starting-pressure ratio as a function of ejector inlet Mach number is shown in figure 12. Experimental data for straight-tube and second-throat ejectors from the present investigation and from the two-dimensional diffuser data of references 2 to 5 are presented. A single point is also included from the hot firing run made with a 5000-pound-thrust rocket engine using a 25:1-area-ratio, 15°-conical exhaust nozzle. The second-throat ejector for this run had an $s/D_{ej} = 0.2$, $\delta = 6°$, $\psi = 2.14$, $l/d_{t,2} = 6.0$, and 2:1-area-ratio subsonic diffuser. A theoretical starting line calculated from one-dimensional normal-shock theory is also included. The experimental nitrogen second-throat ejector data presented are for an ejector configuration having a 6° contraction angle and a second-throat $l/d_{t,2}$ of 6 to 8 with a 2:1-area-ratio subsonic diffuser. A single data point is included for the configuration having the lowest operating-pressure ratio. This configuration has a contraction angle δ of 3° with the same second-throat length and subsonic diffuser as for the other configurations presented. Another data point is included for the starting-pressure ratio with the bell nozzle and similar ejector configuration. The contraction ratios for the data presented here are shown in figure 11.

E-485

Figure 12 indicates that starting-pressure ratios considerably below one-dimensional theory were obtained both for the three-dimensional second-throat ejector data of the present investigation and for the two-dimensional diffuser data of reference 5. Starting-pressure ratios for the data of reference 2 were about equal to the one-dimensional theory, probably because of the use of a second throat having zero length. The present investigation indicates at least for the Mach number range from 5 to 6 that considerable improvement in starting-pressure ratio results from second throats having length-to-diameter ratios of about 6.0. A single tailed point at Mach number 7.2 from reference 5 also indicates that starting-pressure ratios below one-dimensional theory are possible for configurations with parallel-walled second throats. The straight-tube ejector starting-pressure ratios of the present investigation were slightly higher than one-dimensional theory. Ejector inlet Mach numbers of the present investigation were based on the geometric ejector-inlet-to-nozzle-throat area ratios and one-dimensional theory. Mach numbers of reference 5 were based on Pitot-tube pressure measurements at the diffuser inlet.

E-485

CQ-2

Figure 12 can be used to estimate the performance of second-throat ejectors that have γ values different from 1.4, if the figure is entered with a value of M_{e_j} based on the actual nozzle or ejector area ratio and γ of 1.4. Although only one data point obtained with a hot firing rocket engine is available to check this procedure, reasonable accuracy is assumed for values of γ between 1.3 and 1.4.

SUMMARY OF RESULTS

The following results were obtained in an experimental model study of two zero-flow ejector types:

1. A minimum chamber-to-ambient starting-pressure ratio of about 23 was obtained for both bell and 15°-conical 25:1-area-ratio nozzles with a straight-tube ejector having a length-to-diameter ratio of about 8 and an ejector-to-nozzle-throat area ratio of 28.

2. A subsonic diffuser with a 2:1 area ratio attached to the end of the straight-tube ejector had the effect of lowering the starting-pressure ratio from about 23 to 22.

3. A reduction in the starting-pressure ratio of 23 for the straight-tube ejector to 13.5 for the second-throat ejector, or about 41 percent, was obtained by use of a second-throat ejector with a contraction angle of 6°, a contraction area ratio of 2.14, and an ejector overall-length-to-maximum-diameter ratio of 8.

4. The minimum second-throat ejector starting-pressure ratio occurred with a 6° convergent angle and with a second-throat length-to-diameter ratio of about 6 to 8.

5. Maximum experimental second-throat contraction area ratios that permit ejector selection over a wide range of ejector inlet Mach numbers are given.

6. Ejector performance is given which permits estimating starting-pressure ratios for a range of ejector inlet Mach numbers.

E-485

Lewis Research Center
National Aeronautics and Space Administration
Cleveland, Ohio, September 25, 1959

REFERENCES

1. Fortini, Anthony: Performance Investigation of a Nonpumping Rocket-Ejector System for Altitude Simulation. NASA TN D-257, 1959.

2. Diggins, J. L., and Lange, A. H.: A Systematic Study of a Variable Area Diffuser for Supersonic Wind Tunnels. NAVORD Rep. 2421, U.S. Naval Ord. Lab., Dec. 1952.

3. Moore, John A.: Investigation of the Effect of Short Fixed Diffusers on Starting Blowdown Jets in the Mach Range from 2.7 to 4.5. NACA TN 3545, 1956.

4. Bertram, Mitchel H.: Investigation of the Pressure-Ratio Requirements of the Langley 11-Inch Hypersonic Tunnel with a Variable-Geometry Diffuser. NACA RM L50I13, 1950.

5. Wegener, Peter P., and Lobb, R. Kenneth: NOL Hypersonic Tunnel Number 4 Results II; Diffuser Investigation. NAVORD Rep. 2376, U.S. Naval Ord. Lab., May 5, 1952.

6. Shapiro, Ascher H.: The Dynamics and Thermodynamics of Compressible Fluid Flow. Vol. II. Ronald Press Co., N. Y., 1953, pp. 1153-1156.

7. Ames Research Staff: Equations, Tables, and Charts for Compressible Flow. NACA Rep. 1135, 1953. (Supersedes NACA TN 1428.)

E-485
CQ-2 back

TABLE I. - EJECTOR CONFIGURATIONS

[$A_{e,3}/A_{ej}$ or $A_{e,3}/A_{t,2}$, 2.0; θ, 8°.]

(a) Straight-tube ejectors

Nozzle	ϵ	$A_{ej}/A_{t,1}$	L/D_{ej}	Subsonic diffuser
15° Conical	25:1	28	2 to 16	With and without
	25:1	33	2 to 16	↓
	25:1, 50:1	51	2 to 9	↓
Bell	25:1	28	2 to 9	Without
	↓	33	2 to 16	↓
	↓	51	2 to 16	↓

(b) Second-throat ejectors with subsonic diffuser

Nozzle	ϵ	$A_{ej}/A_{t,1}$	ψ	s/D_{ej}	δ, deg	$l/d_{t,2}$
15° Conical	25:1	30	2.48	0.18 to 3.2	3, 6	0 to 10.0
	↓	↓	2.32	0	6	6.0
	↓	↓	2.14	0 to 3.2	3, 6, 15	0 to 10.0
	↓	↓	1.84	.18 to 3.2	↓	↓
	↓	↓	1.66	0 to 3.2	↓	↓
	50:1	57	2.48	0.13 to 1.64	6	6.0
	↓	↓	2.32	.13 to .63	↓	↓
	↓	↓	2.14	.13 to 1.64	↓	↓
Bell	25:1	30	2.48	0.18 to 3.2	3, 6	0 to 10.0
	↓	↓	2.14	.18 to 3.2	3, 6, 15	↓
	↓	↓	1.84	0 to 3.2	↓	↓
	↓	↓	1.66	0 to 3.2	↓	↓

Ni
fl

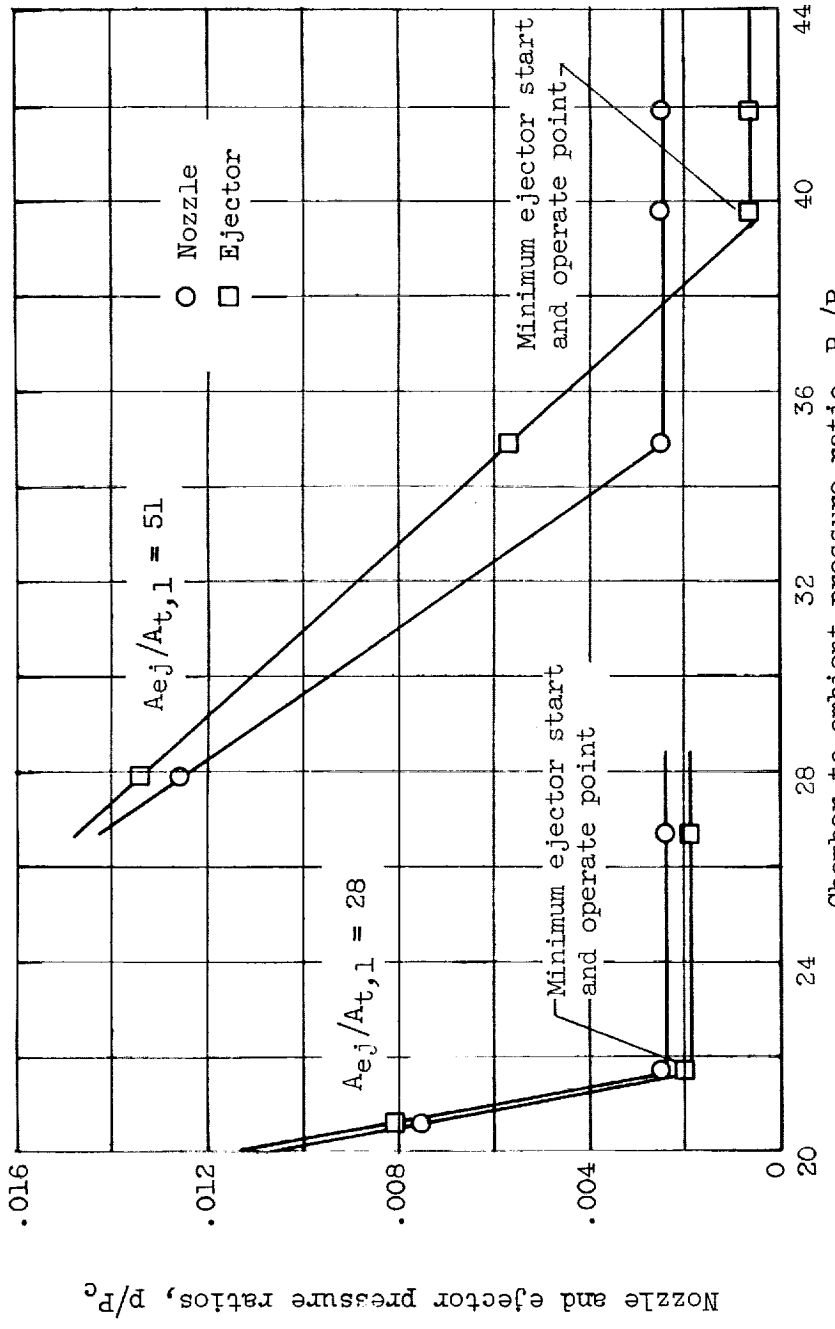

Figure 3. - Typical straight-tube ejector performance. 15^o Conical nozzle; ε, 25:1; L/D_{ej}, 6 to 9.

E-485
CQ-2 back

TABLE I. - EJECTOR CONFIGURATIONS

[$A_{e,3}/A_{ej}$ or $A_{e,3}/A_{t,2}$, 2.0; θ, 8°.]

(a) Straight-tube ejectors

Nozzle	ϵ	$A_{ej}/A_{t,1}$	L/D_{ej}	Subsonic diffuser
15° Conical	25:1	28	2 to 16	With and without
	25:1	33	2 to 16	↓
	25:1, 50:1	51	2 to 9	↓
Bell	25:1	28	2 to 9	Without
	↓	33	2 to 16	↓
	↓	51	2 to 16	↓

(b) Second-throat ejectors with subsonic diffuser

Nozzle	ϵ	$A_{ej}/A_{t,1}$	Ψ	s/D_{ej}	δ, deg	$l/d_{t,2}$
15° Conical	25:1	30	2.48	0.18 to 3.2	3, 6	0 to 10.0
	↓	↓	2.32	0	6	6.0
	↓	↓	2.14	0 to 3.2	3, 6, 15	0 to 10.0
	↓	↓	1.84	.18 to 3.2	↓	↓
	↓	↓	1.66	0 to 3.2	↓	↓
	50:1	57	2.48	0.13 to 1.64	6	6.0
	↓	↓	2.32	.13 to .63	↓	↓
	↓	↓	2.14	.13 to 1.64	↓	↓
Bell	25:1	30	2.48	0.18 to 3.2	3, 6	0 to 10.0
	↓	↓	2.14	.18 to 3.2	3, 6, 15	↓
	↓	↓	1.84	0 to 3.2	↓	↓
	↓	↓	1.66	0 to 3.2	↓	↓

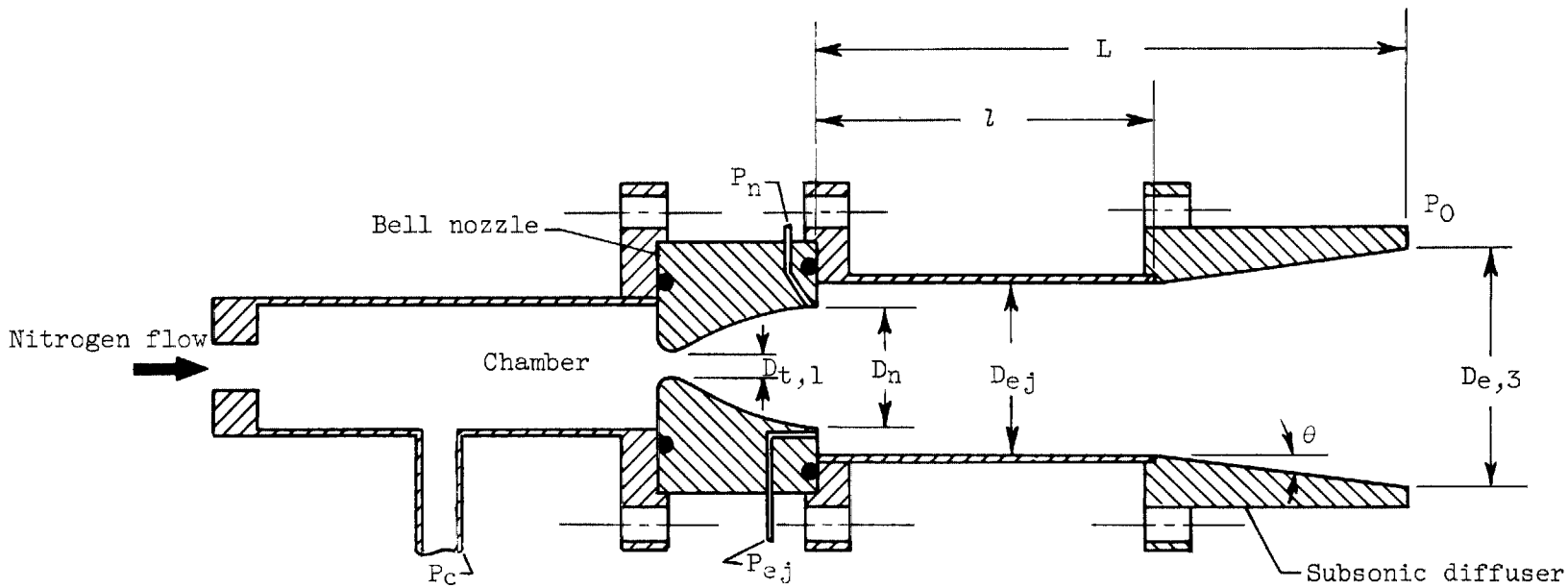

Figure 1. - Straight-tube-ejector test apparatus.

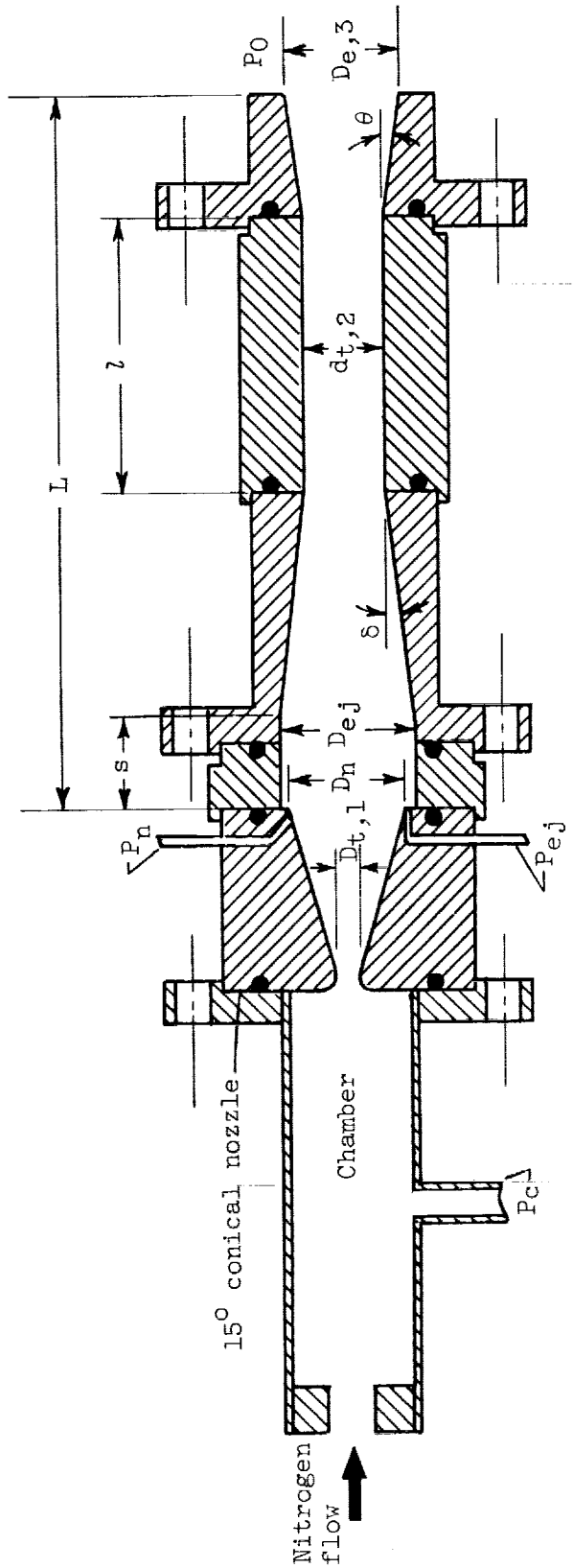

Figure 2. - Second-throat-ejector test apparatus.

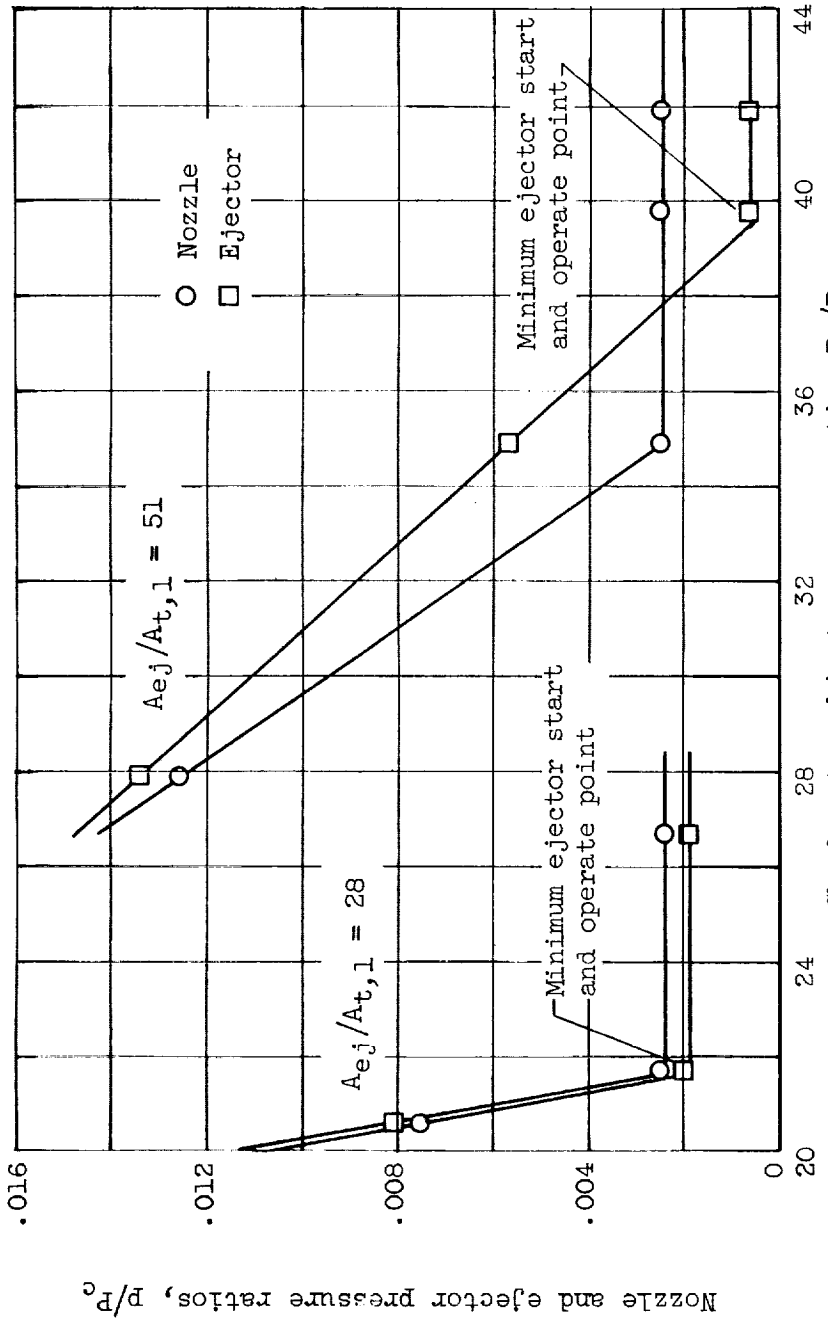

Figure 3. - Typical straight-tube ejector performance. 15° Conical nozzle; ϵ, 25:1; L/D_{ej}, 6 to 9.

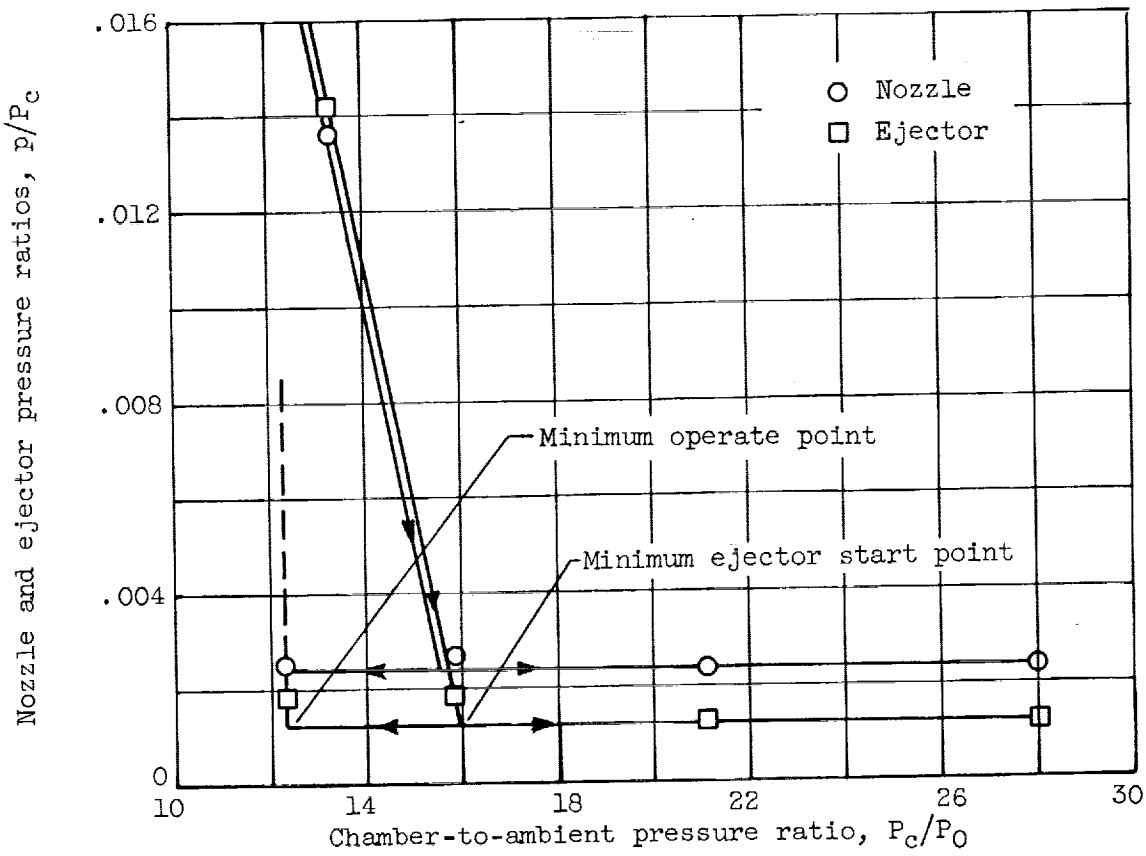

Figure 4. - Typical second-throat ejector performance. 15° Conical nozzle; δ, 3°; ψ, 2.14; L/D_{ej}, 8.

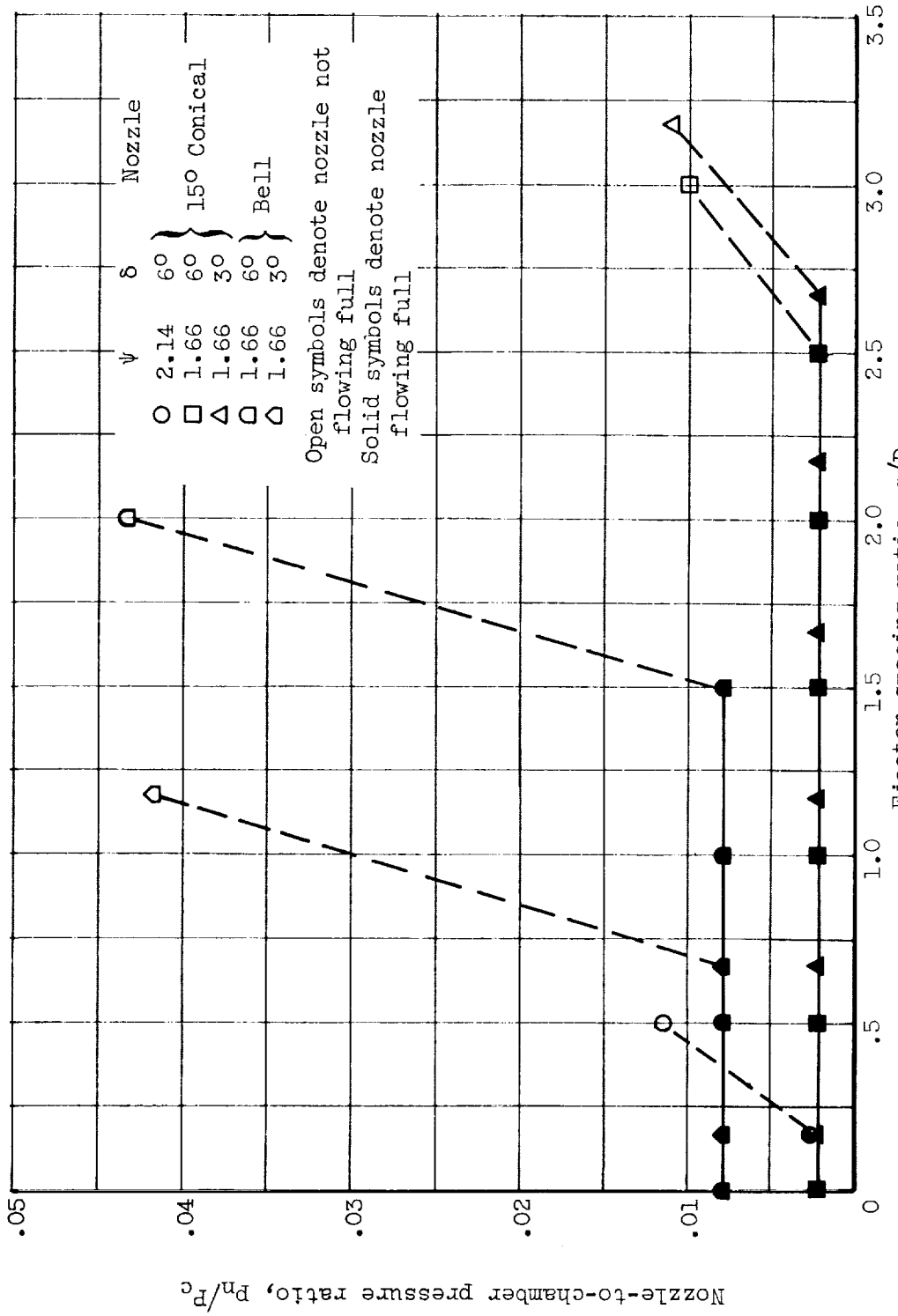

Figure 7. - Effect of ejector spacing ratio on nozzle starting-pressure ratio for second-throat ejectors.

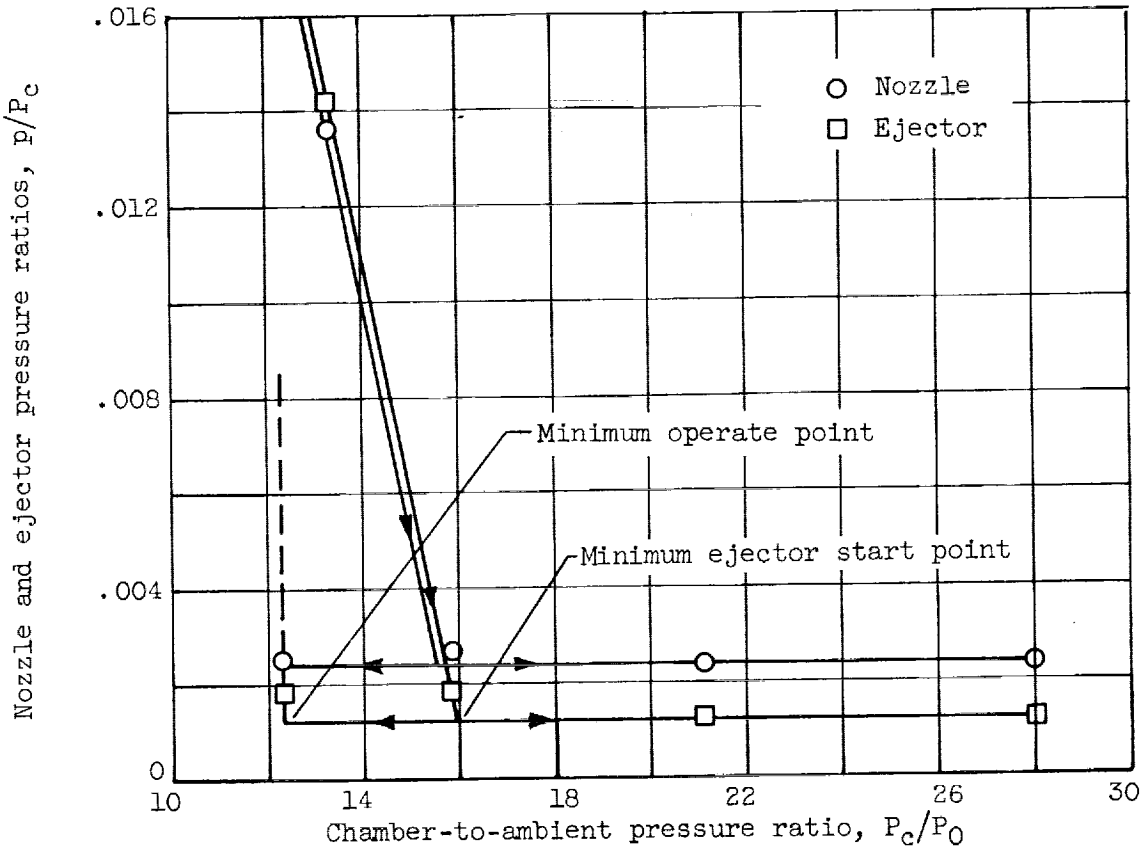

Figure 4. - Typical second-throat ejector performance. 15° Conical nozzle; δ, 3°; ψ, 2.14; L/D_{ej}, 8.

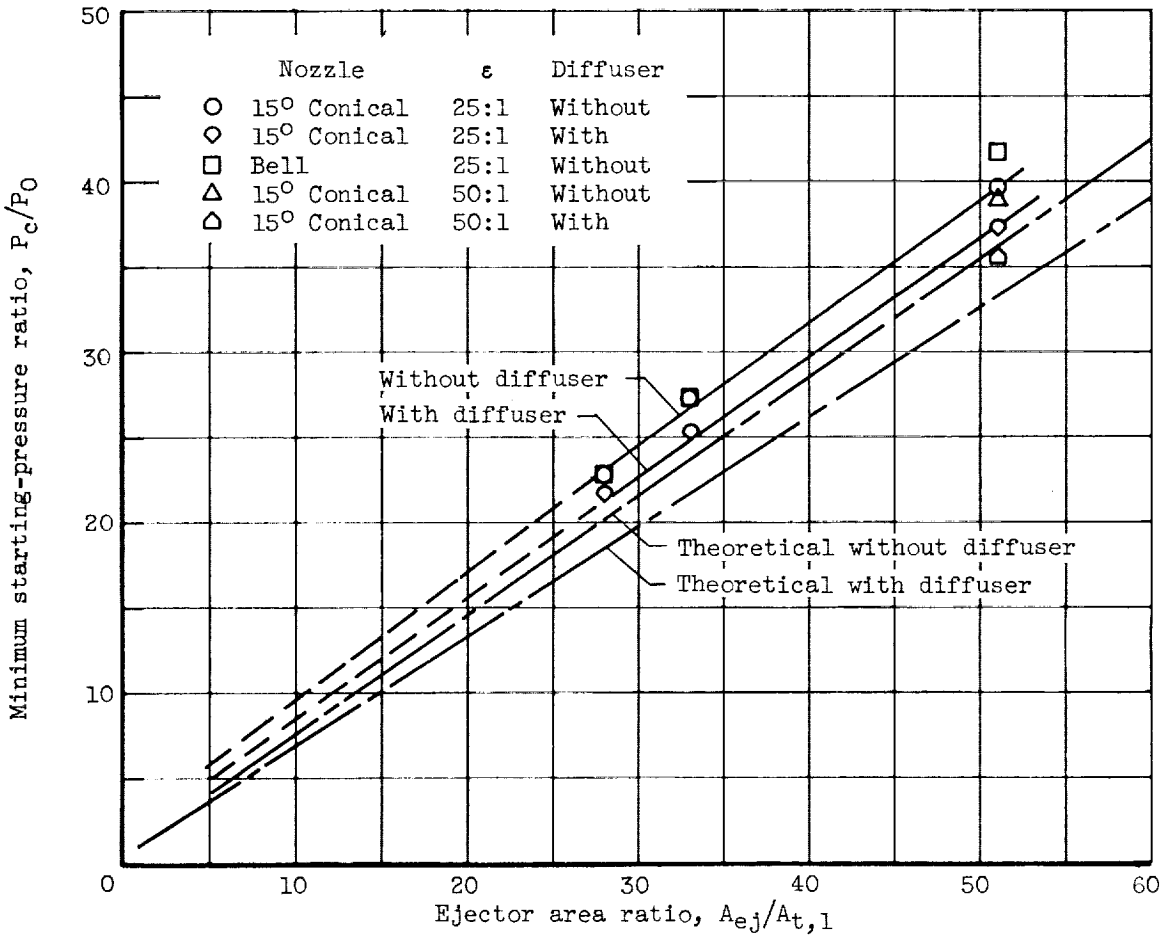

Figure 5. - Effect of ejector area ratio on minimum ejector starting-pressure ratio for three straight-tube ejectors. L/D_{ej}, 8 to 10.

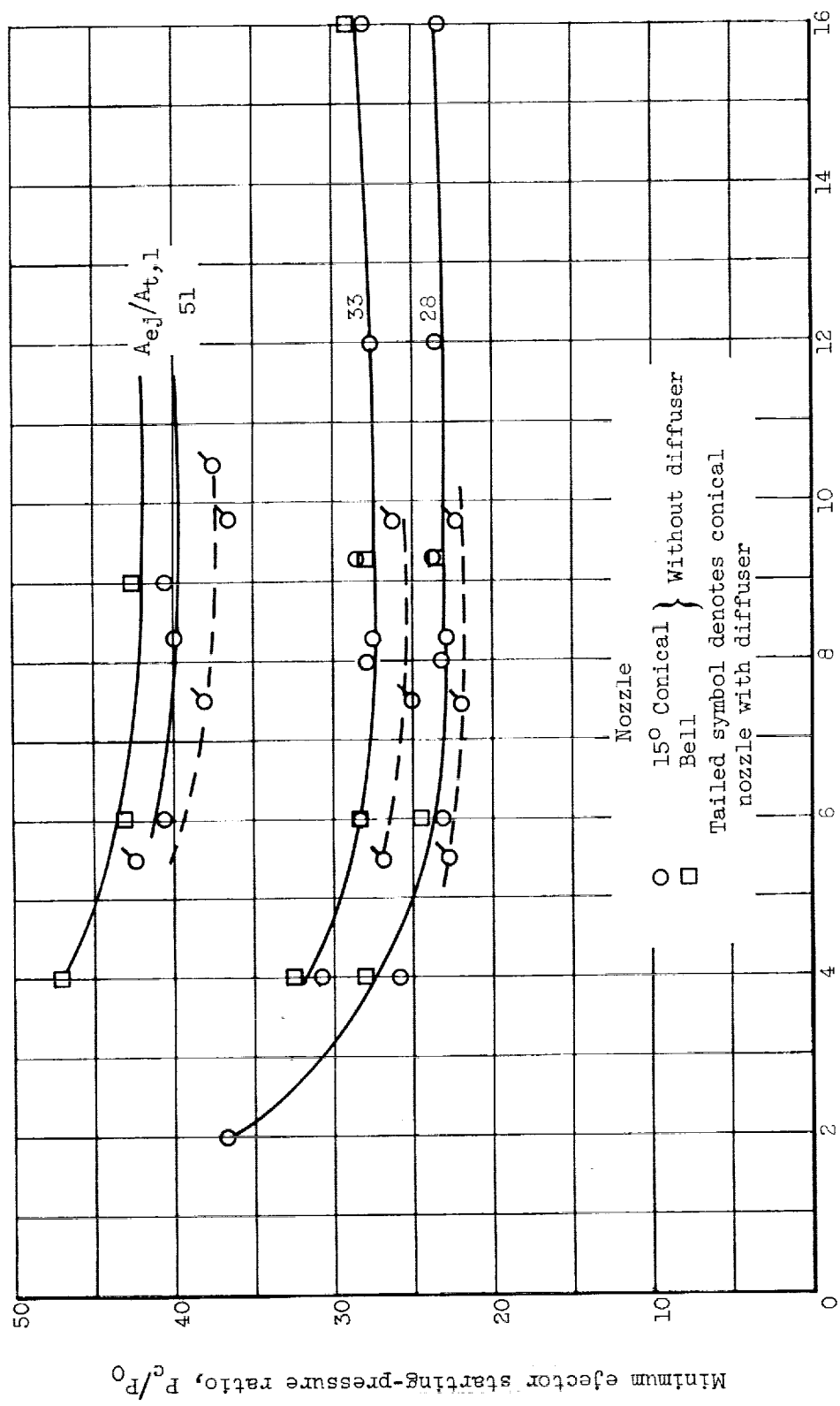

Figure 6. - Effect of ejector overall-length-to-diameter ratio on ejector minimum starting-pressure ratio for straight-tube ejectors. Nozzle area ratio, ε, 25:1.

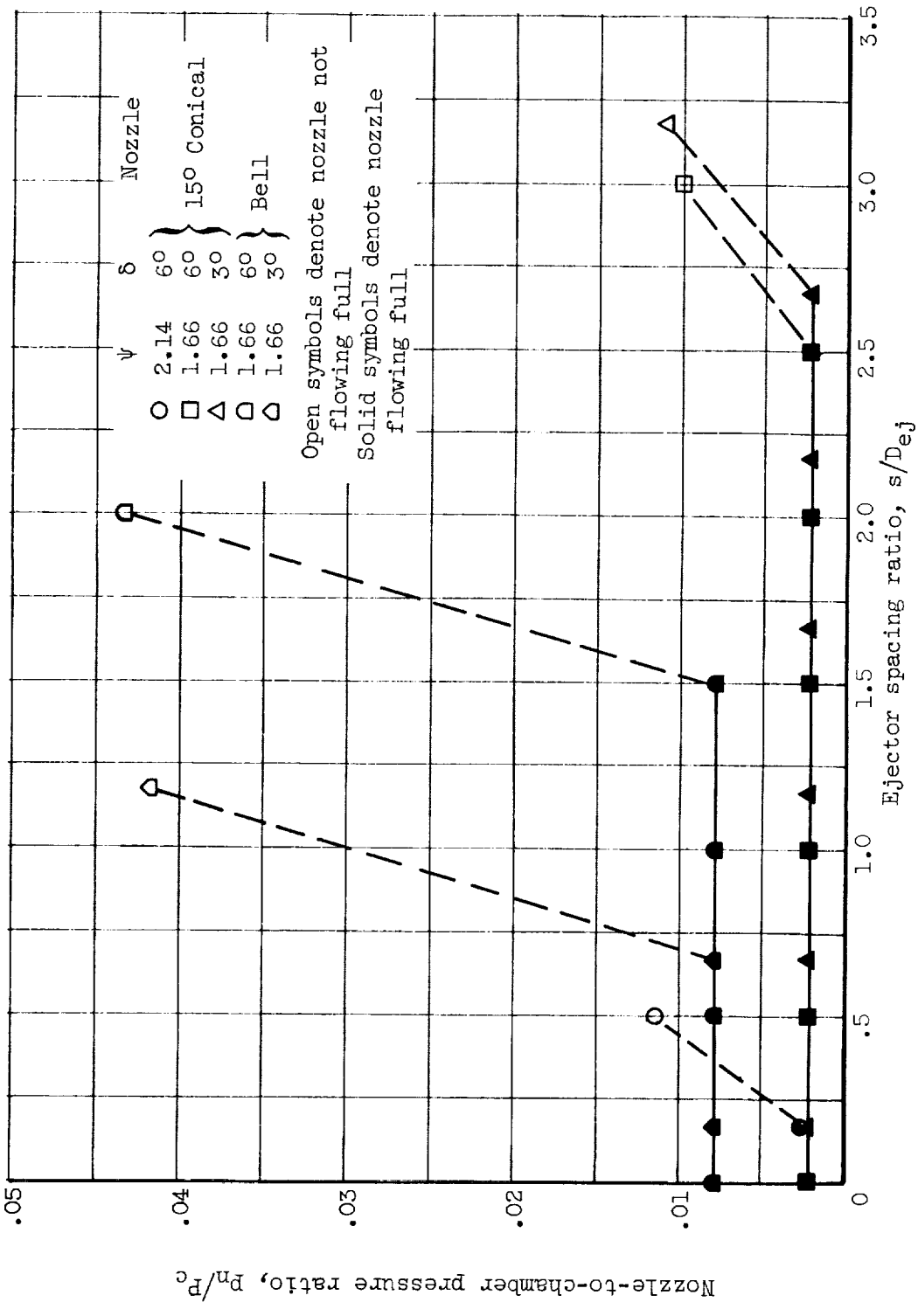

Figure 7. - Effect of ejector spacing ratio on nozzle starting-pressure ratio for second-throat ejectors.

E-485

CQ-3 back

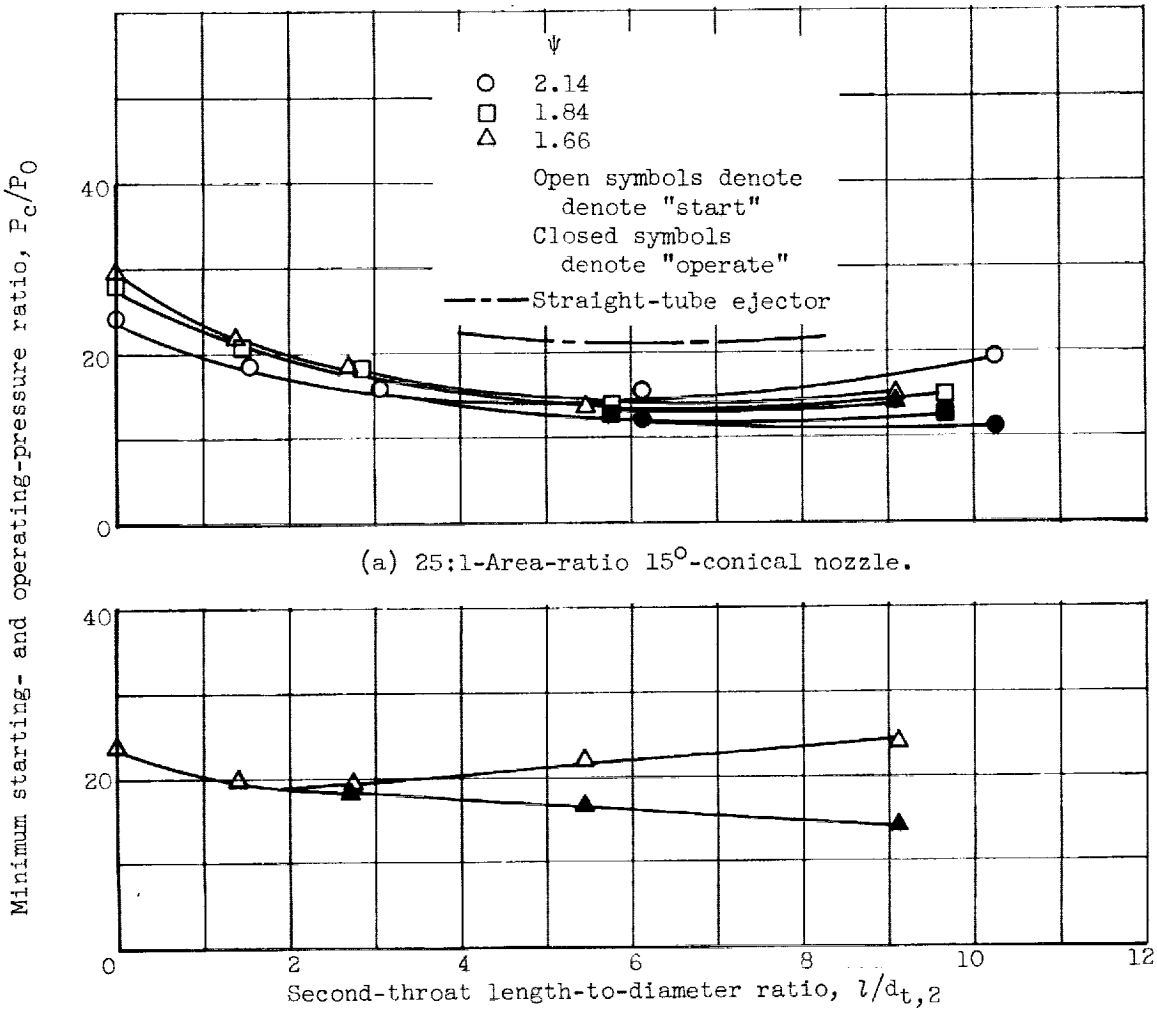

Figure 8. - Effect of second-throat length-to-diameter ratio on second-throat ejector performance. Contraction angle, δ, 3°; $A_{ej}/A_{t,1}$, 30; $A_{e,3}/A_{t,2}$, 2; ϵ, 25:1.

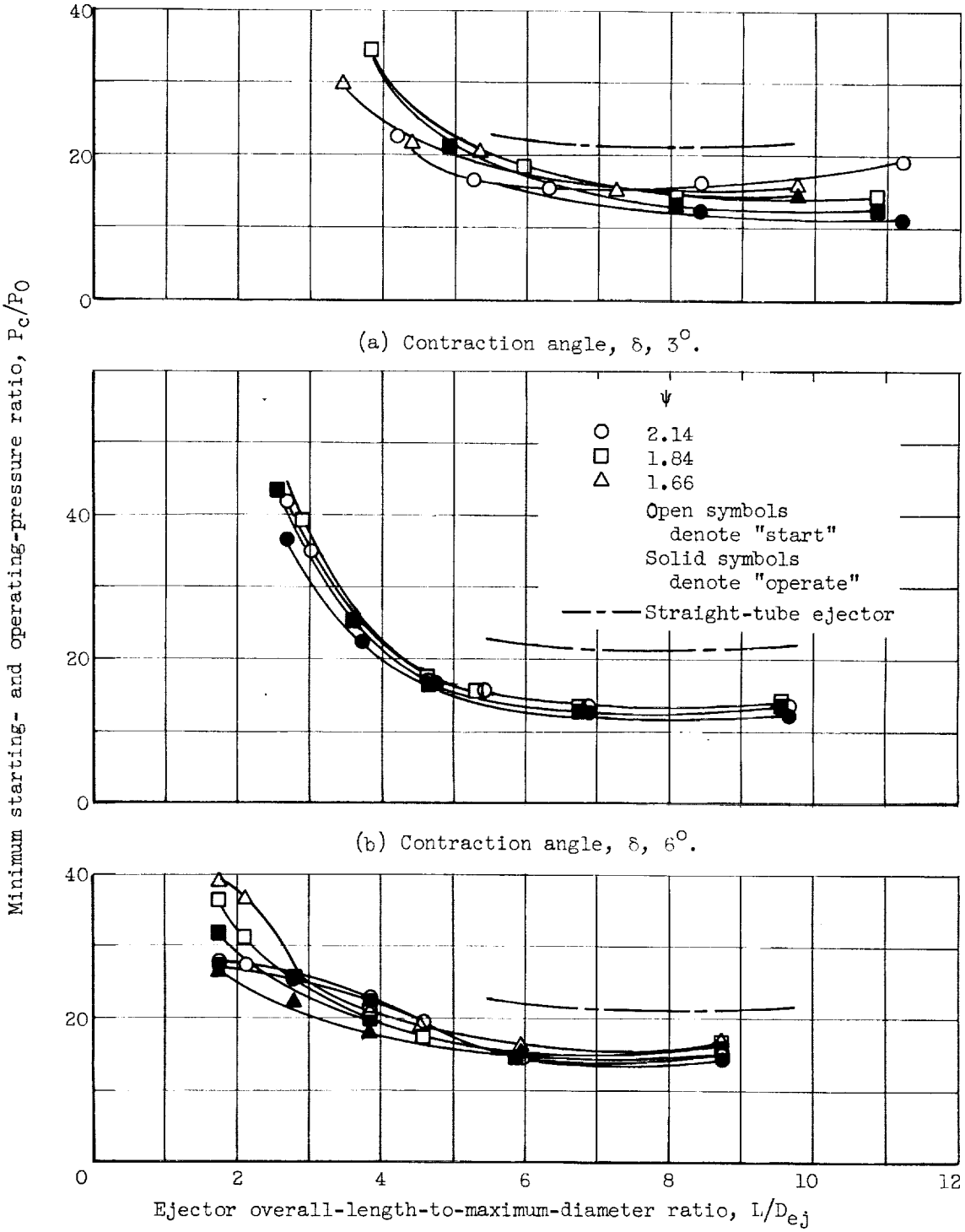

Figure 9. - Effect of ejector overall-length-to-maximum-diameter ratio on ejector performance for second-throat ejector with conical 25:1-area-ratio primary nozzle. $A_{ej}/A_{t,1}$, 30; $A_{e,3}/A_{t,2}$, 2.

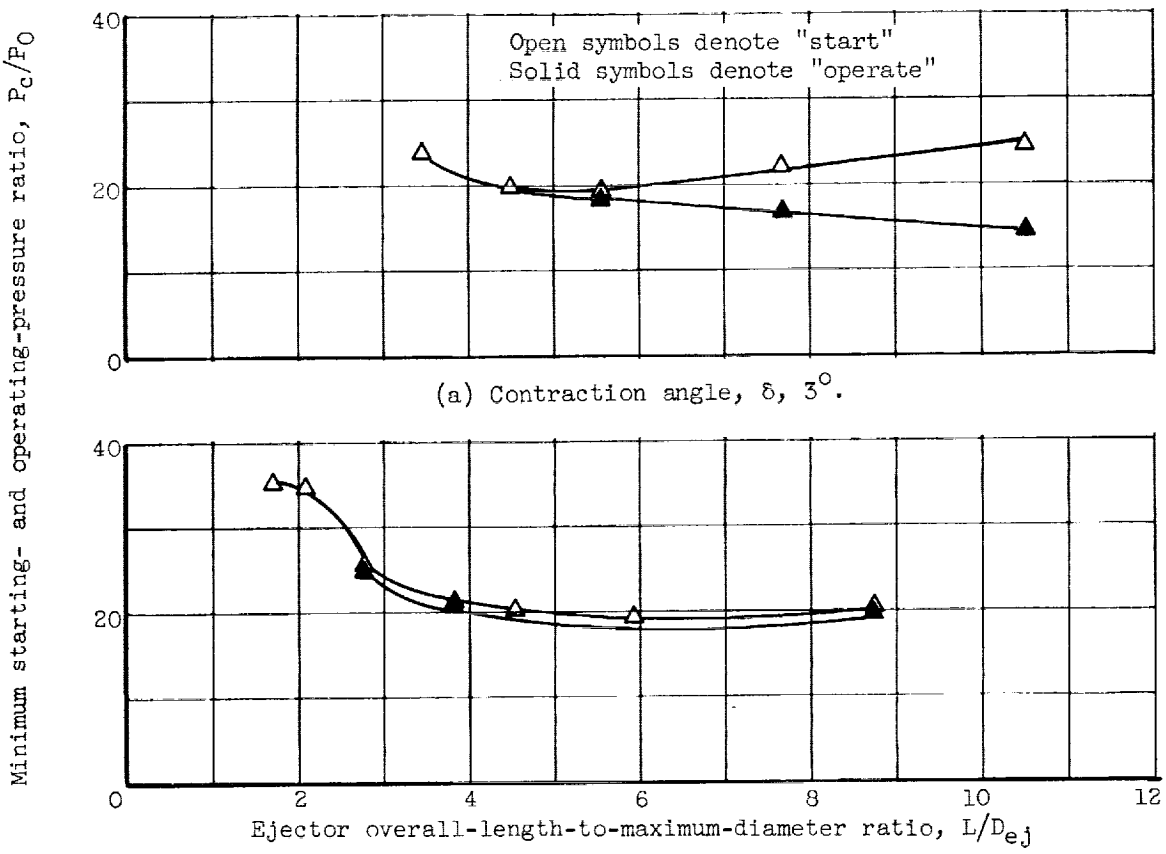

Figure 10. - Effect of ejector overall-length-to-maximum-diameter ratio on ejector performance for second-throat ejector with bell 25:1-area-ratio primary nozzle. Contraction area ratio, ψ, 1.66; $A_{ej}/A_{t,1}$, 30; $A_{e,3}/A_{t,2}$, 2.

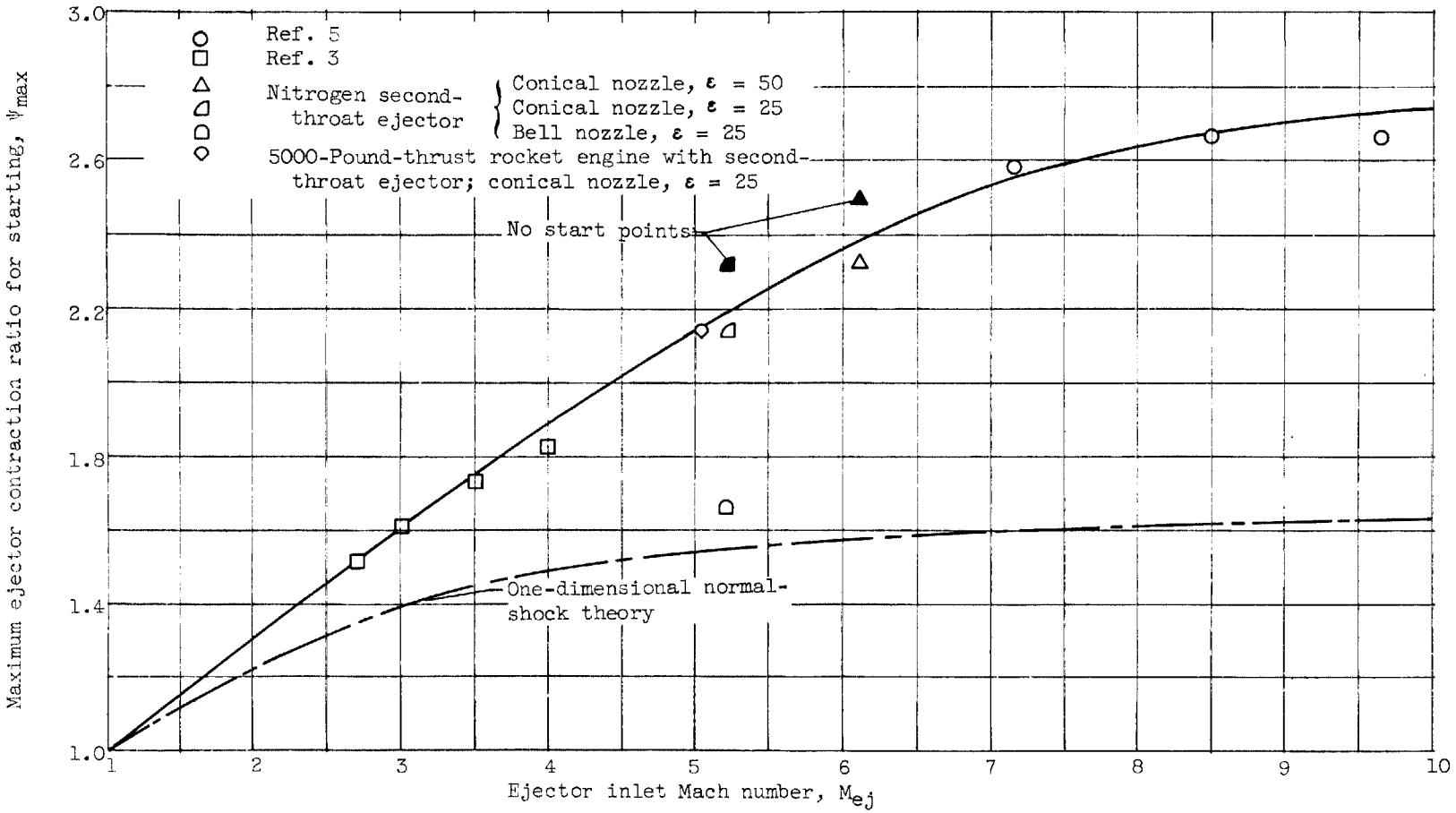

Figure 11. - Effect of ejector inlet Mach number on maximum contraction ratio for starting.

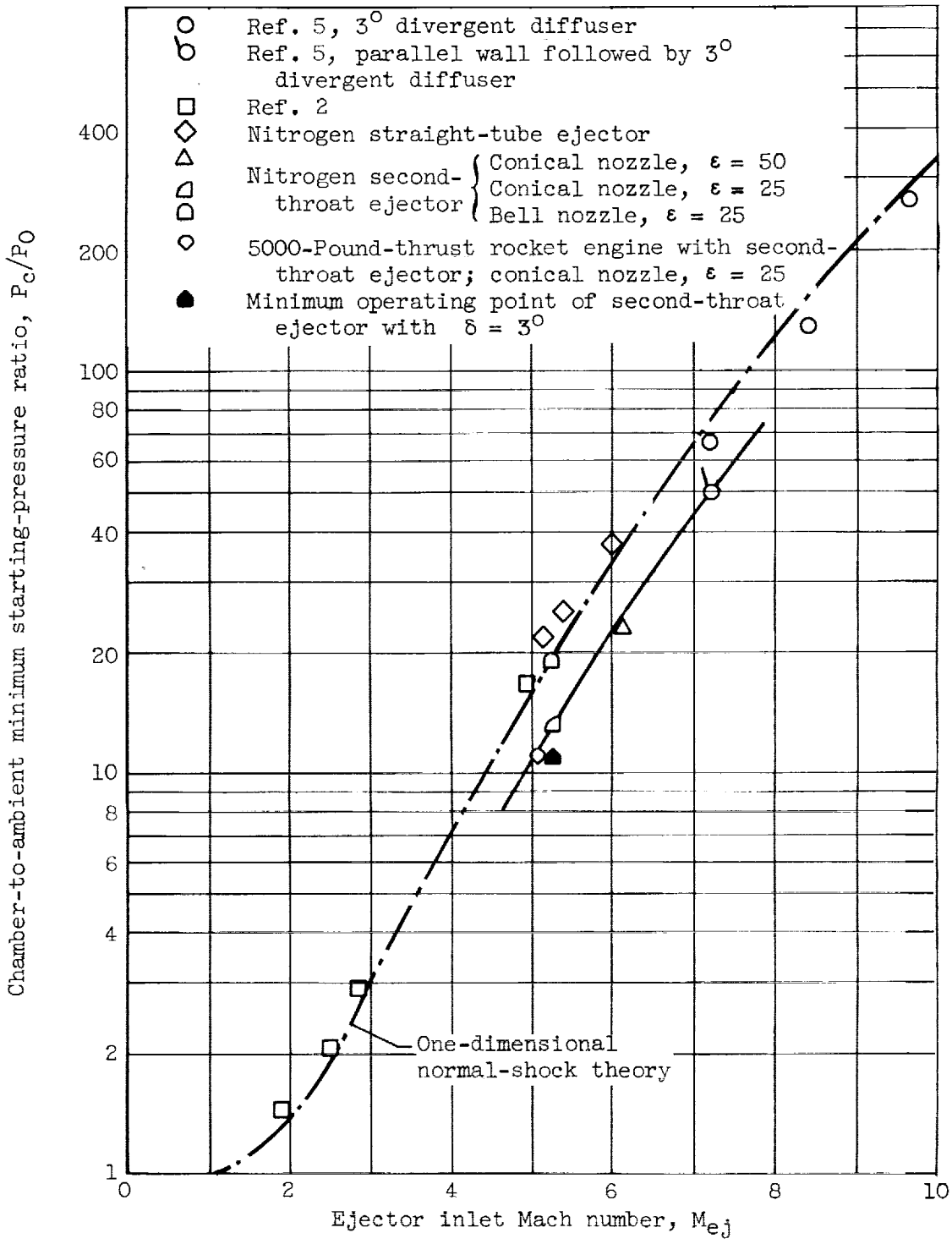

Figure 12. - Effect of ejector inlet Mach number on ejector starting-pressure ratio; γ, 1.4.